RAPID COMMUNICATIONS

PHYSICAL REVIEW A VOLUME 37, NUMBER 9 MAY 1, 1988

Measurements of electron temperature in x-ray heated plasmas

R. Kodama, M. Kado, K. A. Tanaka, A. Yamauchi, T. Mochizuki,* T. Yamanaka, S. Nakai, and C. Yamanaka
Institute of Laser Engineering, Osaka University, 2-6 Yamada-Oka, Suita, Osaka, 565 Japan
(Received 14 December 1987)

Experimental study is presented of an electron temperature in an intense soft-x-ray heated plasma through extreme ultraviolet spectroscopy. Temperatures obtained from time integrated x-ray line and continuum emissions were found to be $T_e = 53 I_x (10^{13}\ \mathrm{W/cm^2})^{0.29}$(eV) for Al plasma over the range of intensities of 10^{12} to 6×10^{12} W/cm^2. The intensity scaling of temperature is compared with an analytical model and is found to agree well with this model.

Recent experiments have shown that a shorter wavelength laser converts its energy efficiently to x-ray energy.[1,2] The energy transport has been found to be mostly carried out by sub-keV x rays in high-Z matter irradiated at interest (a few times 10^{14} W/cm$_2$) laser intensities.[2,3] Thus, it becomes particularly important to understand the x-ray interaction with a solid matter. In addition to such basic physical processes, a study of x-ray heating of solid matter is also practically important for various applications using intense x rays such as x-ray backlighting, x-ray lithography, and x-ray laser with a photopumping scheme. In such application, there are unavoidable problems in that the x-ray-irradiated objects are heated by the x rays of unnecessary photon energy components. There have been a few experimental studies about intense x-ray interaction with solid matter which were published in open literature.[4]

In this paper, we present measurements of an electron temperature of x-ray-heated Al plasma for the first time.[5] Soft x rays penetrate into a high-density region and heat up a certain volume, resulting in the lowering of the temperature of heated plasmas (e.g., 100 eV).[4] By Al K-shell diagnostics we cannot measure such a relatively low temperature because it was shown that the line intensity ratios formed from lines from H-like and He-like ions provided plasma temperatures of more than about 300 eV.[6] Even if some temperatures were measured by the line, often too weak, those temperatures could be erroneous since these lines could result from local hot spots. Here, we obtained temperatures of x-ray-heated plasmas through extreme ultraviolet (XUV) spectroscopy which has measured L-shell line emissions and continuum emissions from Al plasma. The temperature scaling with x-ray intensity was found over the range of intensities of 10^{12} to 6×10^{12} W/cm^2. This scaling agrees well with a simple self-regulating model taking account of the x-ray mean free path.

The experiments have been conducted by using two parallel-plate targets as shown in Fig. 1. 0.53-μm laser light was first focused onto a Au plate (50-μm thickness) through an aspheric lens of $f/1.6$ in a pulse duration of 400 psec (full width at half maximum) with an incidence angle of 54°. The laser intensity on the Au plate was fixed at $(1-2)\times10^{14}$ W/cm^2 in an effective spot diameter of 200 μm. An Al square plate (500×700-μm side length and 50-μm thickness) was used as a target irradiated by x rays from Au plasma and was placed parallel to the Au plate. The Al plate was positioned such that neither the incident laser light nor the specularly reflected light was allowed to heat it directly. An x-ray pinhole camera was used to monitor if the incident laser light directly heated Al plate. The gap distance between the parallel plates was varied from 300–700 μm to control the x-ray intensity.

X-ray spectral measurements were performed using a flat-field grazing incidence XUV spectrometer with a grating of 1200 grooves/mm average pitch whose spectral range was from 45 to 250 Å.[7] The spectrometer has a 50-μm entrance pinhole and a spectral resolution of 0.3 Å for the incidence x-ray wavelength of 60 Å. The spatial resolution was about 50 μm. The spectrometer was mounted at the right angle to the normal direction of the parallel plates and spatially resolved perpendicular to the target plane (see Fig. 1). The time-integrated XUV spectrometer was recorded on a Kodak-type 101 film.[8] A temporal behavior of soft-x-ray emissions was monitored by using two-channel Al photocathode biplanar x-ray diodes (XRD) with a 2-μm-thick parylene and 1-μm Al filters which provided spectral sensitivities in the photon energy range of 0.1–0.3 and 0.6–1.0 keV, respectively.[3] The overall time response of the detector was 350 psec. The XRD's were mounted at a right angle to the normal of the parallel plates (see Fig. 1).

Time-integrated soft-x-ray spectra from Au plasmas were measured separately by 10-channel XRD's at the same laser condition as the one in this experiment but without the lower Al plate. The conversion efficiency defined as the ratio of a measured x-ray energy to the incident laser energy was (25–30)% in 0.1 to 1.6 keV for the

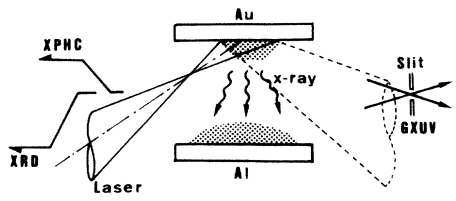

FIG. 1. Experimental setup: Au and Al plates are used as an x-ray emitter and a target irradiated by x rays. XPHC: x-ray pinhole camera. XRD: a set of filtered x-ray diodes. GXUV: flat-field grazing incidence XUV spectrometer.

cosine distribution of the emission. This value was also in reasonable agreement with previous experimental results.[1,3] The x-ray intensity on the Al plate was controlled by the distance between the x-ray emitter (Au) and Al plate and was determined by the illumination geometry. The x-ray spectra and intensity at Au plasmas were kept fixed through this experiment in order to avoid any change in the x-ray absorption processes.

Other energy fluxes such as (1) plasma ion particles, (2) hot electrons from Au plasma, and/or (3) radiation from the stagnated plasma between the parallel plates may heat the Al plate. However, the first two kinds of components (1 and 2) were estimated to be four or more orders of magnitude less than the radiative energy flux from charge collector and x-ray p-i-n diode signals.[3] Moreover, effects of ion components will be reduced by the plasma stagnation between the parallel plates. From the spatially resolved XUV spectra, it was observed that the Au plasma was not stagnated directly on the Al plate but halfway to the Al plate. X-ray emissions from the stagnated plasma were monitored by the XRD's and x-ray intensity was small (typically $< 20\%$ of the x-ray intensity from laser-heated region). Only the radiative energy flux from the laser-heated Au plate is a major heating flux to the Al plate.

An example of XUV spectra on 50–100 Å from x-ray heated Al plasmas obtained with two different x-ray intensities is shown in Fig. 2. It should be noted that the continuum spectral peak shifts to a higher-energy side with increase of incident x-ray intensity. These observed characteristics are caused by the change of the averaged ionization state with the increased electron temperature since the free-bound spectrum is a function of the ionization state.[9] For a Boltzmann distribution of free electrons, we can estimate the average ionization state from the spectral peak.

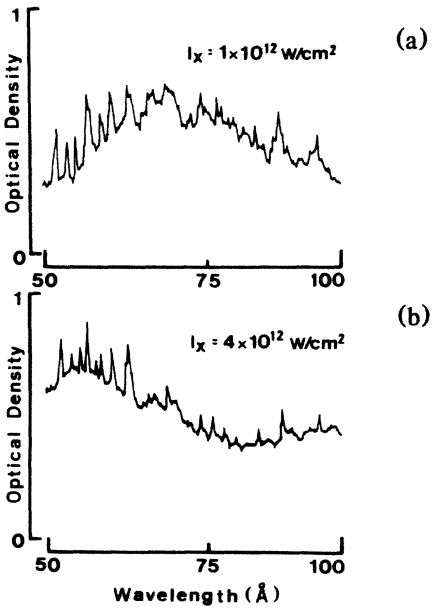

FIG. 2. XUV spectra from x-ray-heated Al plasmas with different x-ray intensities I_x. (a) $I_x = 1\times10^{12}$ W/cm². (b) $I_x = 4\times10^{12}$ W/cm².

Bold bars in Fig. 3 show temperatures versus x-ray intensity from the continuum spectra or average ionization state. The correlation of the electron temperature and the average ionization state by the hybrid-atom model (HAM) (Ref. 10) were used in order to determine the electron temperature. This model is a combination of the collisional-radiative model and the averaged-ion model. The correlation also depends on the ion density which was estimated to be $0.1-1.0\times10^{19}$ cm^{-3} from the intensity ratio of the L-shell line emissions. In these L-shell emissions, the transitions of Al^{8+} $2s^22p^2(3P)-2s^22p3d(3D)$ and Al^{8+} $2s2p^3(5S)-2s2p^23d(5P)$ (Ref. 11) were used. The width of the temperature value in Fig. 3 is due to the uncertainty of the ion density.

Triangles in Fig. 3 show electron temperatures obtained from a temperature-sensitive L-shell ratio [Al^{10+} $2s^2-2s3p(1P)$ and Al^{11+} $2p-3s$].[11] The line intensity ratio depends only slightly ($\leqq \pm 20\%$) on the plasma density between 10^{17} and 10^{21} ions/cm^3 whose magnitude is consistent with experimental data. However, the opacity effects to the L-shell line emissions in such a density region may not be neglected so that radiation transport should be taken into account for determining the temperature. We assumed that an Al plasma with radius of 50–500 μm was produced along the viewing axis of XUV spectrometer in order to consider the opacity effect.[11] The vertical bars are due to the difference of plasma volume or optical thickness. The result from the line ratio is in good agreement (within 20%) with that from the ionization state. It is readily seen in Fig. 3 that the electron temperature increases with the x-ray intensity. The scaling suggested by our data is $T_e = 53\times I_x(10^{12}\ \mathrm{W/cm^2})^{0.29}$(eV), where I_x is incident x-ray intensity on Al plate.

If we assume a steady state for x-ray heated plasmas, the electron temperature could be estimated by considering a self-similar isothermal expansion from the Chapman-Jouguet (C-J) point.[12,13] In this model, the x-ray intensity is

$$I_x = 4m_i n_{is} C_s^3 + U_r + U_i \ , \tag{1}$$

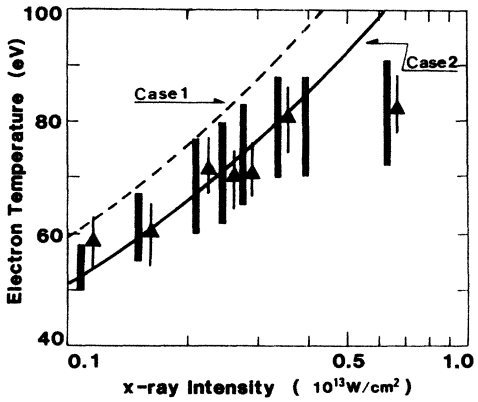

FIG. 3. Temperature vs x-ray intensity for x-ray-heated Al plasmas. Bold bars and triangles show the temperatures estimated from continuum spectra and line ratio. Dashed (case 1) and solid (case 2) lines are temperature scalings from analytical models. Case 2 includes the ionization loss into case 1.

where U_r, U_i, and C_s are the radiative loss (reemission in the deflagration region), the ionization loss, and the sound speed $C_s \simeq \sqrt{ZT_e/m_i}$, respectively. m_i and n_i are the ion mass and density. $4m_i n_{is} C_s^3$ is the heat flux necessary to maintain a self-similar isothermal expansion in which case the outward heat flux is $m_i n_{is} C_s^3$ and the inward flux is $3m_i n_{is} C_s^3$.[12]

At first approximation (case 1), we neglected the ionization loss and the radiation loss as $I_x = 4m_i n_{is} C_s^3$. The inward energy flux of reemission U_r' is assumed to be less than the energy flux necessary to form the deflagration as $U_r' < 3m_i n_{is} C_s^3$. The structure and thickness of the ablation region are approximated by a radiation mean free path L_r. It is a reasonable assumption that the electron thermal conduction is neglected in the deflagration region, comparing the mean free paths of thermal electron with that of x-ray radiation. Moreover, L_r and $n_i(x)$ are assumed to have forms such as $L_r(x) = f(T_e)g(n_i) = f(T_e)/n_i(x)^2$ and $n_i(x) = n_{is}\exp(-x/C_s\tau)$, respectively; also, the energy density of reemission in the deflagration region is assumed to be negligibly small compared to that of the incident radiation. The ion density at the C-J point is given from diffusion approximation[14] for the radiation flux as

$$n_{is} = [\ln(\tfrac{4}{3})/\sqrt{3}\times 2f(T_e)/C_s\tau]^{1/2} , \tag{2}$$

where τ is the duration of the radiation pulse.[13] In the absorption process of radiation, the plasma is assumed to be in equilibrium condition ($T_e = T_r$). But in the emission process, the plasma may be out of the equilibrium condition, namely, the emissivity of reemission is much smaller than that in the case of the blackbody condition. A quasiequilibrium condition such as this might be reasonably assumed as long as x-ray pulse continues, since the x-ray produced plasma at the C-J point will have a low temperature and high density. Then a simple scaling of the temperature is obtained from Eqs. (1) and (2) taking account of the relation of $L_r = aT_e^{3/2}T_r^2/[n_i^2 Z(Z+1)^2]$ with $a = 4.4\times 10^{22}$ cm^{-5}deg$^{7/2}$ for bound-free radiation[14] as

$$T_e = 1.36\times 10^{-1}[I_x^{12/35}(\mathrm{W/cm^2})][(\tau^2 AA'^{1/3})]^{3/35}\ (\mathrm{eV}) , \tag{3}$$

where we assume the relation of $Z = \frac{2}{3}(A'T_e)^{1/3}$.[15] Here, A and A' are the atomic weight and the atomic number, respectively. This scaling as shown in Fig. 3 for dashed line is about 30% higher than the experimental results. Such a result may stem from the neglect of the ionization loss U_i and/or radiation loss U_r in Eq. (1).

Next (case 2), we considered the ionization loss and the thermal energy is written from Eq. (1) as

$$I_x - U_i = 4m_i n_{is} C_s^3 = I_x \frac{3/2kT_e(Z+1)}{3/2kT_e(Z+1)+\sum\chi_n} = (0.6\text{–}0.7)I_x , \tag{4}$$

where χ_n is the ionization potential.

The scaling taking account of ionization loss is shown as a solid line in Fig. 3. This scaling is in good agreement with the experimental result over the x-ray intensity of 10^{12} to 4×10^{12} W/cm^2. This comparison implies that the incident radiation over such intensity will be quasiequilibrated with the plasma.

It should be also noted that the saturation of temperature is found at a x-ray intensity of more than 5×10^{12} W/cm^2. There are some possible mechanisms for the saturation. Considering the temperature at the ion density of 10^{19} cm^{-3}, the radiation loss is one of the important factors used to determine the electron temperature. Al plasma has a peak of emissivity by L-shell emission at the electron temperature of about 100 eV.[11] Thus, the effect of radiation losses through L-shell emission will be essential to the temperature scaling near 100 eV and the temperature may be saturated around 100 eV.[16]

The ionization burnthrough in the x-ray absorption process may also be one of the factors saturating the electron temperature.[4,17] The photon energy of 100–300 eV of incident radiation is a component which forms about 30% of incident x-ray energy, and is mainly absorbed through the Al L-absorbed edge. However, temperature rise shifts the ionization front. Thus, incident radiation with the same energy flux penetrates further into a higher density region and heats a rather large volume, resulting in the temperature saturation. Details of saturation mechanisms are beyond our scope and should be studied in the future.

In summary, we have measured the electron temperature of intense x-ray-heated Al plasma through XUV spectroscopy. The temperature scaled with x-ray intensity as $T_e = 53I_x(10^{13}\ \mathrm{W/cm^2})^{0.29}$ (eV) over the range of intensity of 10^{12} to 4×10^{12}. Temperature scaling is also obtained with a simple self-regulating model taking account of the x-ray mean free path. Good agreement is found when we assume that the radiation is quasiequilibrated with plasma considering the ionization loss. Saturation of temperature at around $T_e \sim 100$ eV suggests a radiation loss by L-shell emission and/or ionization burnthrough in the absorbed region.

The authors would like to acknowledge the technical assistance of N. Doi and H. Nakano. The target fabrication by the members of the Target Group is gratefully acknowledged.

*Present address: Research and Development Center, Hoya, Musashino 3-3-1, Akishima, Tokyo, 196 Japan.

[1] W. C. Mead, E. M. Campbell, K. G. Estabrook, R. E. Turner, W. L. Kruer, P. H. Y. Lee, B. Pruett, V. C. Rupert, K. G. Tirsell, G. L. Stradling, F. Ze, C. E. Max, M. D. Rosen, and B. F. Lasinski, Phys. Rev. Lett. **47**, 1289 (1981); H. Nishimura, F. Matsuoka, M. Yagi, K. Yamada, S. Nakai, G. H. McCall, and C. Yamanaka, Phys. Fluids **26**, 1688 (1983).

[2] W. C. Mead, W. L. Kruer, R. E. Turner, C. W. Hatcher, D. S. Bailey, P. H. Y. Lee, J. Foster, K. G. Tisell, B. Puett, N. C. Holmes, J. J. Trainor, G. L. Stradling, B. F. Lasinski, C. E. Max, and F. Ze, Phys. Fluids **27**, 1301 (1984); R. F. Schmalz, J. Meyer-ter-Vehn, and R. Ramis, Phys. Rev. A **34**, 2177 (1986).

[3]R. Kodama, K. Okada, N. Ikeda, M. Mineo, K. A. Tanaka, T. Mochizuki, and C. Yamanaka, J. Appl. Phys. **59**, 3050 (1986); T. Mochizuki, T. Yabe, K. Okada, M. Hamada, N. Ikeda, S. Kiyokawa, and C. Yamanaka, Phys. Rev. A **33**, 525 (1986).

[4]T. Mochizuki, K. Mima, N. Ikeda, R. Kodama, H. Shiraga, K. A. Tanaka, and C. Yamanaka, Phys. Rev. A **36**, 3279 (1987).

[5]R. Kodama *et al.*, in The Sixth APS Topical Conference on Atomic Processes in High Temperature Plasmas and the International Conference, Santa Fe, New Mexico, 1987 (unpublished), p. 4B-3.

[6]H. J. Kunze, A. H. Gabriel, and H. R. Griem, Phys. Rev. **65**, 267 (1968); U. Feldman, G. A. Doschek, D. K. Prinz, and D. Nagel, J. Appl. Phys. **47**, 1341 (1976); D. Duston and J. Davis, Phys. Rev. A **21**, 1664 (1980).

[7]T. Kita, T. Harada, N. Nakano, and H. Kuroda, Appl. Opt. **22**, 512 (1983); N. Nakano, H. Kuroda, T. Kita, and T. Harada, *ibid.* **23**, 2386 (1984).

[8]B. L. Henke, S. L. Kwok, J. Y. Uejio, H. T. Yamada, and G. G. Young, J. Opt. Soc. Am. B **1**, 818 (1984).

[9]H. Griem, *Plasma Spectroscopy* (McGraw-Hill, New York, 1964); R. W. P. McWhirter and F. Stratton, in *Plasma Diagonostic Techniques,* edited by R. H. Huddlestone and S. L. Leonard (Academic, New York, 1965); D. Mosher, Phys. Rev. A **10**, 2330 (1974).

[10]M. Ito and T. Yabe, Phys. Rev. A **35**, 233 (1987); M. Ito, Masters thesis, Osaka University, 1987 (unpublished).

[11]D. Duston and J. Daivis, Phys. Rev. A **23**, 2602 (1981).

[12]R. E. Kidder, Nucl. Fusion **14**, 797 (1974); H. Takabe, K. Nishihara, and T. Taniuti, J. Phys. Soc. Jpn. **45**, 2001 (1978); P. Mora, Phys. Fluids **25**, 1051 (1982).

[13]K. Nozaki and K. Nishihara, J. Phys. Soc. Jpn. **48**, 993 (1980); K. Nishihara, Jpn. J. Appl. Phys. **21**, L571 (1982); T. Yabe, S. Kiyokawa, T. Mochizuki, S. Sakabe, and C. Yamanaka, *ibid.* **22**, L88 (1982).

[14]Ya. B. Zel'dovich and Yu. P. Raiser, *Physics of Shock Waves and High Temperature Hydrodynamic Phenomena* (Academic, New York, 1966).

[15]D. Colombant and G. F. Tonon, J. Appl. Phys. **44**, 3524 (1973).

[16]S. K. Goel, P. D. Gupta, and D. D. Bhawlkar, J. Appl. Phys. **53** 223 (1982).

[17]D. Duston, R. W. Clark, J. Davis, and J. P. Apruzese, Phys. Rev. A **27**, 1441 (1983).

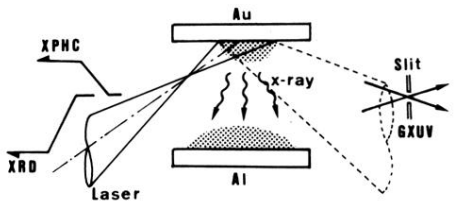

FIG. 1. Experimental setup: Au and Al plates are used as an x-ray emitter and a target irradiated by x rays. XPHC: x-ray pinhole camera. XRD: a set of filtered x-ray diodes. GXUV: flat-field grazing incidence XUV spectrometer.